TiO_2- and $BaTiO_3$-Assisted Photocatalytic Degradation of Selected Chloroorganic Compounds in Aqueous Medium: Correlation of Reactivity/Orientation Effects of Substituent Groups of the Pollutant Molecule on the Degradation Rate

L. Gomathi Devi* and G. Krishnamurthy

Department of Post Graduate Studies in Chemistry, Central College Campus, Dr. Ambedkar Street, Bangalore University, Bangalore-560001, India

Received: April 13, 2010; Revised Manuscript Received: October 23, 2010

Investigation of the photocatalytic activity of $BaTiO_3$, a perovskite wideband gap semiconductor has been done in comparison with a widely used photocatalyst TiO_2 for the degradation of 4-chlorophenol (4-CP), 4-chloroaniline (4-CA), 3,4-dichloronitrobenzene (3,4-DCNB), and 2,4,5-trichlorophenol (2,4,5-TCP). $BaTiO_3$/TiO_2 nanoparticles were prepared by gel-to-crystalline conversion method. $BaTiO_3$ has exhibited better catalytic efficiency and process efficiency compared with TiO_2 in most of the cases. The present research focuses mainly on two aspects: first the photocatalytic activity of $BaTiO_3$, as there are very few reports in the literature, and second the reactivity/orientation effects of substituent groups of the pollutant molecules on the degradation rate. The above chloroorganic compounds have at least one chlorine substituent in common, along with other functional groups such as $-OH$, $-NH_2$, and $-NO_2$. Furthermore, the effect of electron acceptors and pH on the rate of degradation is presented. The reactions follow first-order kinetics. The degradation reaction was followed by UV−vis, IR, and GC-MS spectroscopic techniques. On the basis of the identification of the intermediates, a probable degradation reaction mechanism has been proposed for each compound.

Introduction

Contamination of the earth's environment by toxic chemicals from various means in a larger extent is a serious threat to the entire world. The contamination of the aquatic environment largely contributes to the total pollution. The present research is pertained to mineralization of water contaminants by advanced oxidation processes (AOPs) using two different semiconductor photocatalysts. In the present research, $BaTiO_3$, a wide band gap perovskite semiconductor photocatalyst is used in comparison with extensively used TiO_2.[1]

The influence of the substituent groups of some selected chloroorganic compounds, especially their position and orientation on the aromatic ring, affects the degradation rate. There are only a few studies on these compounds in this regard.[2] The use of $BaTiO_3$ as photocatalyst for the mineralization of chloroorganic compounds and the influence of substituents is less attempted.[3,4] Therefore, this kind of study may gain separate scope in photocatalysis.

The chloroaromatic compounds such as chlorinated benzenes, phenols, amines, and so on are well-known long persisting pollutants, which contaminate the aqueous environment.[5−7] These chemicals may also be formed by the reaction between naturally occurring chlorine with humic and fulvic substances in the environment. The other sources may be the synthetic chloroorganic compounds, which are used as pesticides, laboratory reagents, and so on. The waste containing these chemicals from the industries and other manufacturing units enter the nature with/without treatment, thereby polluting the environment. Even if they implement effluent treatment, it may not be to the extent of complete mineralization of the toxicants, and thus they do contribute to the environmental pollution. The chlorinated compounds are more stable because of the presence of a strong C−Cl bond. They are all possibly carcinogens. They persist in nature for a longer duration and pollute the aquatic, air, and soil environment. As a mark of awareness in the environmental protection, the researchers have shown interest in degrading such hazardous chlorinated compounds.[8,9] This photochemical advanced oxidation processes of mineralization of toxic compounds in heterogeneous systems on the reactive surfaces, such as titania or metal oxides, is a promising process for the environmental clean up, especially at parts per million concentrations.[10,11]

The degradation of simple aromatic compounds such as 4-chlorophenol (4-CP), 4-chloroaniline (4-CA), 3,4-dichloronitrobenzene (3,4-DCNB), and 2,4,5-trichlorophenol (2,4,5-TCP), which are highly carcinogenic and environmentally hazardous,[12] has been attempted. The aim of selecting the above compounds for the research is to study the effect of the substituents on the aromatic ring and their influence on the rate of degradation. The study also focuses on the aspects of understanding the mechanism of photodegradation via the formation of various intermediate products. In all of these compounds, one of the common substituents is a reactive functional chloro −Cl) group at the para position. For the comparative study, the compounds containing a chloro group at the meta/ortho position in di/trichloro compounds are also chosen. These are mono, di, and trichloro compounds along with different functional groups such as $-OH$, $-NH_2$, and $-NO_2$ groups. The presence of rigid C−Cl bond in the molecule along with the other functional groups makes the molecule more stable. The rate of degradation depends on the nature of substituents, the stability of the molecule, and the type of intermediate compounds formed during the process of degradation.

* Corresponding author. Tel: +91-080-2961336. Fax: +91-080-22961331. E-mail: gomatidevi_naik@yahoo.co.in.

10.1021/jp103301z
Published on Web 12/31/2010

Experimental Section

1. Materials. ***1.1. $BaTiO_3$ and TiO_2.*** Titanium tetrachloride, ammonium hydroxide, sulphuric acid, barium hydroxide, ammonium persulphate, hydrogen peroxide, nitric acid, and sodium hydroxide were all obtained from E-Merck chemicals. The solutions are prepared using distilled water.

1.2. Chloroorganic Compounds. The samples of 4-CP, 4-CA, 3,4-DCNB, and 2,4,5-TCP were obtained from E-Merck chemicals and are used as obtained from the company.

2. Analytical Methods and Characterization of Photocatalysts. TiO_2 and $BaTiO_3$ photocatalysts were prepared by gel-to-crystalline conversion method.[13,14] $BaTiO_3$ is obtained by reaction of gels of hydrated titania with barium hydroxide, as reported by Kutty et al.[14] The recovered solids from both processes were oven-dried at 105−120 °C. $BaTiO_3$ is further annealed at 450 °C, and TiO_2 is further annealed at 600 °C for 4 h.

The above powders were characterized by X-ray diffraction studies.[4] The diffractograms were obtained using Phillips PW 1050/70/76 X-ray diffractometer. The Cu Kα radiation was used with a nickel filter. The scanning range employed was $2\theta = 5-80°$. The normal scanning speed was 2°/min, and the check speed was 2 mm/min. The diffraction pattern shows anatase polymorph for TiO_2 and tetragonal phase for perovskite $BaTiO_3$. The crystallite sizes were obtained using Scherrer's equation ($D_{hkl} = K\lambda/\beta \cos \theta$) relating the pure diffraction breadth (half bandwidth) to the crystallite size normal to the plane $h\ k\ l$, where $D_{h,k,l}$ is the mean dimension in angstroms, λ is the wavelength, β is the pure diffraction line broadening, θ is the Bragg's angle of the reflection $h\ k\ l$, and K is the constant approximately equal to unity.[13] Full width at half-maximum depends on crystallite size and microstrain in the lattice. The crystallite sizes were found to be 17.9 and 19.2 nm for TiO_2 and $BaTiO_3$, respectively.

The particle size is determined by scanning electron microscope (SEM) using JEOL-JSM 840 A. A uniform film thickness of ∼0.1 mm was maintained for both samples. The average particle size of TiO_2 and $BaTiO_3$ from the SEM analysis is found to be 57−251 and 85−286 nm, respectively.

The diffused reflectance spectrum of anatase TiO_2 and $BaTiO_3$[4] was taken using the Shimadzu UV−vis-160 model spectrophotometer. The reflectance data obtained were relative to percentage reflectance with respect to the nonabsorbing material $BaSO_4$, which can optically diffuse the light. According to P. Kubelka and F. Munk theory, the diffused reflectance of the powdered samples for an infinitely thick layer is given by eq 1, as used by Fuller et al.[15]

$$f(R_\infty) = \frac{(1 - R_\infty)^2}{2R_\infty} = \frac{k}{s} \quad (1)$$

where R_∞ is the absolute reflectance of the layer, s is the scattering coefficient, and k is the molar absorption coefficient. The λ_{max} values for TiO_2 and $BaTiO_3$ were found to be 413 and 372 nm, respectively, from Kubelka−Munk plots of relative reflective intensity $(1 - R_\infty)^2/2R_\infty$ versus wavelength, and the corresponding band gaps are 3.0 and 3.3 eV, respectively.

The energy dispersive X-ray (EDX) analysis using the JSM-840A EDX analyzer shows the following results: Ti/O atom % in TiO_2 is found to be 33.25/66.75, and Ba/Ti/O in $BaTiO_3$ is found to be 19.63/20.25/60.12.

The surface area and the pore volume of the catalyst powders by BET method are determined using NOVA-1000 high gas sorption analyzer (Quanta Chrome Corporation) version 3.70. The average pore diameter and the specific surface area for TiO_2/$BaTiO_3$ is found to be 147.18/104.95 Å and 50.54/34.14 m^2/g, respectively.

The degradation reaction was followed by UV−visible spectrophotometer (Shimadzu UV−vis-160 model), FTIR (Nicolet Impact 400 D FTIR), and GC-MS (17A Shimadzu GC-MS QP-5050 A) techniques for analyzing the intermediates.

3. Photocatalytic Degradation Procedure. Photodegradation experiments were carried out in a reaction cell of 1 L capacity with the exposure area of 92.2 cm^2. The experiments are performed by direct exposure of UV-light into the reaction mixture at a height of 29.5 cm in the presence of atmospheric oxygen. A medium pressure 125 W mercury vapor lamp is used as the light source (wavelength ≈ 350−400 nm). The photon flux is found to be 7.76 mW/cm^2, as determined by ferrioxalate actionometry.

Photocatalytic degradation experiments of 4-CP, 4-CA, 3,4-DCNB, and 2,4,5-TCP at 10 ppm concentration have been carried out under UV light in the presence of TiO_2/$BaTiO_3$ catalyst suspensions in ∼0.75 g L^{-1}. The 2000 ppm stock solution of each chloroorganic compound was prepared using methanol. The 10 ppm reaction solution of these compounds was prepared using distilled water from the above stock solution. The reaction solution in all experiments is stirred for 15 min at the rate of 120 rpm before the start of illumination to ensure adsorption of substrate on catalyst particles. The temperature was normally maintained around 25 °C. The samples were withdrawn at different time intervals and centrifuged to remove suspended TiO_2/$BaTiO_3$ particles to analyze residual concentration and the intermediates formed during the process of degradation by various spectroscopic methods.

Results and Discussion

1. Process Efficiency and Catalytic Efficiency. In the heterogeneous photocatalysis it is often very difficult to measure the intensity of the absorbed light accurately and to obtain a value for the quantum yield (Φ) of the photosystem under test.[16,17] Instead, many researchers are content in quoting the formal quantum efficiency ($\Phi = \upsilon_0/I$) for their photosystem, where the quantum efficiency can also be defined in terms of initial rate υ_0 of the reaction and the number of photons (or intensity I of light) absorbed by the reaction system.[18] It is to be noted that the quantum yield for most of the heterogeneous systems is usually much greater than the above formal quantum efficiency because a substantial amount of incident light is often lost to reflection and scattering rather than being absorbed.[19] Therefore, in the present work, the process efficiency η as an alternate has been calculated. The process efficiency ($\eta = C_0 - C/tIS$) is defined as the change in the concentration per time divided by the amount of the energy in terms of intensity of light and the exposure surface area,[20] where C_0 is the initial concentration of the substrate and C is the concentration at anytime t. The term ($C_0 - C$) represents the change in the concentration in mg L^{-1} or ppm at any time t (min), I is the intensity of the light in Einstein s^{-1} m^{-2}, and S is the exposure surface area in m^2.

The rate of photocatalytic degradation primarily depends on the generation of e^-−h^+ pairs and their involvement in the oxidation/reduction process. In addition to this, the rate of formation of several reactive species such as O_2^-, O_2^{2-}, $^{\cdot}OH$, and so on in the aqueous solution also determines the rate of photodegradation.[21,22] In turn, the production of these reactive

radicals depends on the number of photons absorbed by the system. These events can be represented by the following equations.

$$BaTiO_3/TiO_2 + h\upsilon \rightarrow e^-_{cb} + h^+_{vb} \quad (2)$$

$$O_2 + e^-_{cb} \rightarrow {}^{\cdot}O_2^- \quad (3)$$

$$O_2^- + e^-_{cb} \rightarrow O_2^{2-} \quad (4)$$

$$H_2O + h^+_{vb} \rightarrow {}^{\cdot}OH + H^+ \quad (5)$$

$$OH^- + h^+_{vb} \rightarrow {}^{\cdot}OH \quad (6)$$

where e^-_{cb} is the conduction band electron and h^+_{vb} is the valence band hole. The time taken for complete mineralization of 4-CP, 4-CA, 3,4-DCNB, and 2,4,5-TCP under UV-irradiation with various experimental conditions is given in the Table 1. The process efficiency values calculated for the degradation of these chloroorganic compounds in the presence of both of the photocatalysts are given in Table 2.

The catalytic efficiency ($C_{eff} = k/C_{cat}$) of the photocatalyst is the ratio of the apparent rate constant for the degradation process to the concentration of the catalyst, where C_{eff} is the catalytic efficiency in L mg^{-1} h^{-1}, k is the rate constant (h^{-1}), and C_{cat} is the concentration of the catalyst in mg L^{-1}. The catalytic efficiency and process efficiency of $BaTiO_3$ is higher than that of TiO_2 (except in the case of 4-CA).

The higher reactivity of $BaTiO_3$ can be due to: (i) the coordination environment of the surface atoms, (ii) red-ox properties of the oxide, and (iii) oxidation state of the metal ions. These factors may be more favorable, for $BaTiO_3$ compared with the TiO_2. Another important factor that can influence the degradation rate is pH, which in turn can influence the catalytic efficiency and process efficiency. The pH of the solution is found to be high ($\sim$ 8.5) in $BaTiO_3$ suspensions compared with TiO_2 suspensions (slightly acidic or neutral), which can alter the band edge positions of the semiconductor particles, directly influencing the rate of degradation.

The catalytic efficiency and the process efficiency are found to be high for the degradation of 4-CA with TiO_2 as the photocatalyst in the presence of H_2O_2. The reason could be the acidic pH ($\sim$5.5), at which the TiO_2 surface possesses more positive charges. The 4-CA molecules get effectively adsorbed from the negative end (NH_2^- of the 4-CA) on the positively charged catalyst surface by the electrostatic force of attraction. Because the adsorption is one of the important parameter that enhances the interfacial charge transfer process in the heterogeneous photocatalysis, the rate of degradation increases. Furthermore, the presence of electron acceptors like H_2O_2 traps the conduction band electrons, which effectively suppress the recombination rate, which additionally contributes to the overall enhancement in the process. Therefore, a higher rate of degradation for 4-CA is observed on the TiO_2 surface.

2. Effect of pH and Oxidizing Agent. ***2.1. Effect of pH.*** Semiconductor (TiO_2/$BaTiO_3$) particles suspended in water behave similar to diprotic acids. The adsorptive properties of these particles depend significantly on the solution pH. At lower pH, the catalyst surface will be positively charged and hence preferentially attracts and adsorbs anionic species. At higher pH, the surface becomes negatively charged, favoring the adsorption of cationic species on the surface. The ions such as Cl^-, HCO_3^-, and SO_4^{2-} can be adsorbed on the positively charged catalyst surface by electrostatic attraction, leading to competitive adsorption.

A series of experiments has been carried out to study the effect of pH on the degradation rate of 4-CP, 4-CA, 3,4-DCNB, and 2,4,5-TCP. The initial pH of the solutions was adjusted using 1 M H_2SO_4/HNO_3 and 1 M NaOH solutions in each case. However the pH maintenance was not done during the process of degradation.

The alkaline pH in the presence of APS/H_2O_2 is found to be favorable for the faster degradation of all these compounds in the presence of both the catalysts. The results can be better understood by taking into account both the surface states of titania and the ionization state of the substrate molecule.[23] The hydroxylated TiO_2 surface can be protonated under acidic medium and deprotonated under alkaline conditions since its point of zero charge (pzc) is $\sim$6.25. In our study, moderate degradation rate was observed in a slightly acidic pH ($\sim$5.5, as prepared solution) in the TiO_2 suspensions. The decrease in the degradation rate of these compounds with TiO_2 shows the following order of pH: $\sim 11 > \sim 5.5 > \sim 2$.

The pH of as-prepared $BaTiO_3$ suspensions is found to be 8.8 and drops to 8.2 after the addition of H_2O_2 in the presence of UV light. Higher rates of degradation were observed with the addition of APS as an oxidant with $BaTiO_3$ in all of the cases except TCP, where both of the catalysts show similar efficiencies. This can be attributed to more negative charges on the $BaTiO_3$ particle surface, which create a better coordination environment for the molecular adsorption. Further alkaline pH may alter the band edge positions of the semiconductor, which results in the faster degradation of the molecules. Under alkaline conditions, excess hydroxyl radicals are generated by the hydroxyl anions in the solution under UV illumination. The acidic pH does not show any significant effect on the rate of degradation, whereas the experiments under alkaline conditions show higher efficiency in the case of $BaTiO_3$.

2.2. Effect of Oxidizing Agents. Photocatalytic oxidation of organic pollutants in the presence of oxidizing agents mainly involves the generation and subsequent reaction of hydroxyl radicals. The hydroxyl radicals produced are nonselective and can therefore oxidize all the pollutants.[24,25] In the present study, symmetrical peroxides like H_2O_2 and APS are added as oxidizing agents to enhance the generation of ${}^{\cdot}OH$ radicals, and they also inhibit charge carrier recombination. In the case of APS, sulfate radicals are also produced along with hydroxyl radicals, which may also actively participate in the degradation mechanism. The rate of degradation is found to enhance appreciably in the presence of APS/H_2O_2.

$$S_2O_8^{2-} + e_{CB}^- \rightarrow SO_4^{2-} + SO_4^{-\cdot} \quad (7)$$

$$SO_4^{\cdot -} + H_2O \rightarrow SO_4^{2-} + {}^{\cdot}OH + H^+ \quad (8)$$

3. Kinetics of Degradation. The rate of degradation of the pollutant can be defined in terms of the decrease in the concentration of the substrate (chloroorganic compound) as a function of time. This change in concentration was monitored mainly by UV−visible absorption spectral study. The photocatalytic degradation of these compounds over illuminated aqueous suspensions of TiO_2/$BaTiO_3$ photocatalysts in the presence of atmospheric oxygen can be represented by the following general equation

$$ArXCl_n + O_2 \xrightarrow[\text{UV light}]{T_iO_2/BaTiO_3} \text{intermediates} \rightarrow aCO_2 + bH_2O + nHCL + XY \quad (9)$$

where Ar is an aromatic ring, n is the number of chlorine atoms on the aromatic ring, a and b represent the number of CO_2 and H_2O molecules formed, respectively, and X is substituent groups such as $-OH$, $-NO_2$, and $-NH_2$. XY is the product formed after degradation of $ArXCl_n$ in the solution. Figure 1 represents the C/C_0 (where C and C_0 are the concentrations at $t = t$ and $t = 0$) versus time plots for the TiO_2/H_2O_2 (plot A) and $BaTiO_3$/APS (plot B) systems, respectively, for all of the above-mentioned chloroorganic compounds. These kinds of plots are extensively used to represent the residual concentration during irradiation.[26−29] The irradiation time on the abscissa at which the C/C_0 ratio becomes zero is the time taken for the complete mineralization. The highest rate for the degradation is observed for DCNB in a time period of 0.75 h. The irradiation times for the complete degradation of these compounds are listed in Table 2.

Figure 2 shows the plots of negative logarithmic residual concentration ($-\ln C/C_0$) versus irradiation time. The slopes of the line give k, implying the first-order kinetics in all of the reactions.[30−32] Table 3 gives the calculated rate constants and time taken for complete degradation of 2,4,5-TCP, 4-CA, 4-CP, and 3,4-DCNB in the presence of catalyst and oxidizing agents for chosen efficient systems. In the study of reaction kinetics, the initial rates and initial concentrations are considered.[33−38] The procedure of dealing with initial rates avoids the possible complications due to the interference by products and leads to an order that corresponds to the simplest type of situation, and this order is referred to as order with respect to the concentration or true order.[28]

Because the rate of degradation is found to depend on the substrate concentration (C_{sub}), the first-order photodegradation reaction can fit to the Langmuir−Hinshelwood (L−H) kinetic model[4,30,33,37] for the above chloroorganic compounds and is represented by the following equation

$$v_{LH} = -\frac{dC}{dt} = \frac{k_{obsd}K_{app}C_{sub}}{1 + K_{app}C_{sub}} \quad (10)$$

where v_{LH} is the L−H kinetic rate, K_{app} is the apparent adsorption equilibrium constants, and k_{obsd} is the observed rate constant.

4. Structure and Reactivity. The rate of degradation of these chloroaromatic compounds depends on the reactivity and orientation of the substituent groups on the aromatic ring. Certain groups can activate the benzene ring on direct substitution at ortho and para positions. The other groups (except halogens) on direct substitution at meta position deactivate the ring. In the present studies, the compounds commonly contain one or more $-Cl$ group(s) along with the groups like $-OH$, $-NO_2$, and $-NH_2$, which are mostly para oriented.

The group attached to the benzene ring will affect the stability of the carbocation by dispersing or intensifying the positive charge, depending on its electron-releasing or electron-withdrawing nature and tendency. The groups like $-NH_2$, $-OH$, and so on tend to neutralize the positive charge of the ring (electron-releasing inductive effect), and this dispersal of the charge stabilizes the carbocation. The groups like $-NO_2$, $-Cl$, and so on have an electron-withdrawing inductive effect. This tends to intensify the positive charge and destabilizes the carbocation.[39]

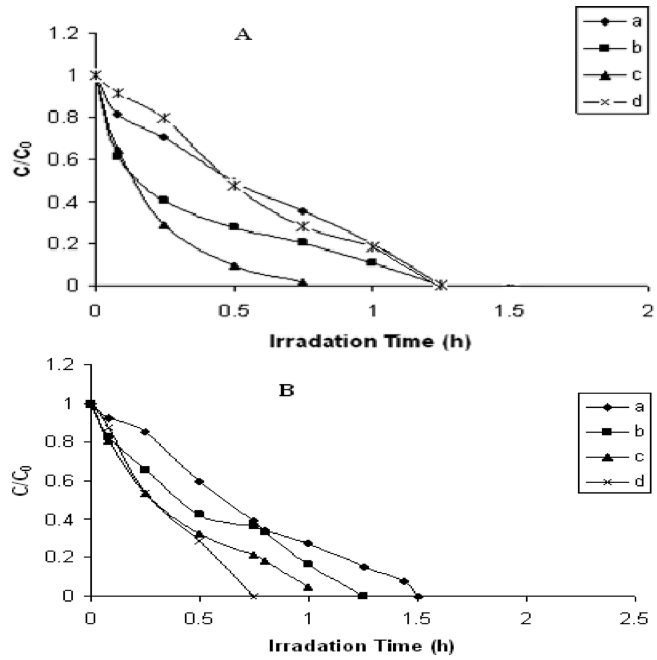

Figure 1. Plots of C/C_0 versus irradiation time for TiO_2 in the presence of H_2O_2 (plot A) and that for $BaTiO_3$ in the presence of APS (plot B) for (a) 4-CP, (b) 4-CA, (c) 3,4-DCNB, and (d) 2,4,5-TCP.

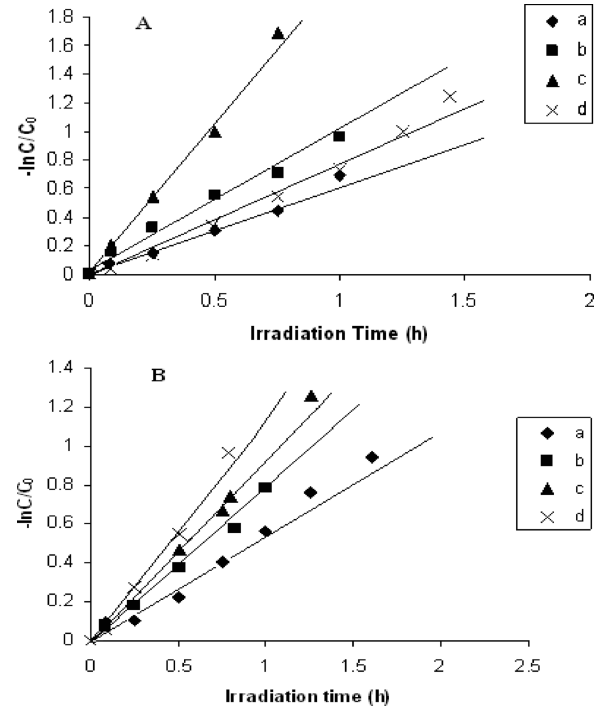

Figure 2. Plots of $-\ln C/C_0$ versus irradiation time for TiO_2 with H_2O_2 (plot A) and that for $BaTiO_3$ in the presence of APS (plot B) for (a) 4-CP, (b) 4-CA, (c) 3,4-DCNB, and (d) 2,4,5-TCP.

A group that releases electrons usually activates the ring, which exactly means that the molecule becomes more stable and resists the degradation, and the group that withdraws electrons deactivates the ring, thereby enhancing the degradation rate. The presence of a greater number of electron-withdrawing groups such as $-Cl$ strongly deactivates the benzene, leading to the faster rate of degradation. However, it is important to note that the halogens are unusual in their effect in stabilizing

TABLE 1: Time Taken for Complete Mineralization of 2,4,5-TCP, 4-CA, 4-CP, and 3,4-DCNB under UV Irradiation with Various Experimental Conditions

expt no.	experimental condition	degradation time (h) TCP	4-CA	4-CP	DCNB
1	solution of compound without catalyst and other reagents (partial degradation)	∼6	∼5	∼5	∼4
2	solution of compound with TiO_2 suspension	2	2.25	2.5	2
3	solution of compound with TiO_2 along with 50 ppm of ammonium persulphate	1.5	1.25	1	1.25
4	solution of compound with TiO_2 along with 20 ppm of hydrogen peroxide	1.25	0.75	1.25	1.25
5	solution of compound with $BaTiO_3$ suspension	2.75	2.5	2.5	2
6	solution of compound with $BaTiO_3$ along with 50 ppm of ammonium persulphate	1.5	1.25	1	0.75
7	solution of compound with $BaTiO_3$ along with 20 ppm of hydrogen peroxide	1.5	1.5	1.25	1.5
8	solution of compound with only ammonium persulphate	4.5	3.75	3.75	3.25
9	solution of compound with only hydrogen peroxide	5.0	4.25	4.0	3.5

TABLE 2: Catalytic Efficiency (CE) and Process Efficiency (PE) Values for the Photocatalytic Degradation of 2,4,5-TCP, 4-CA, 4-CP, and 3,4-DCNB in the Presence of TiO_2/$BaTiO_3$ Catalysts and $(NH_4)_2S_2O_8$ (50 ppm)/H_2O_2(20 ppm) for Experiments 1−7 As Mentioned in Table 1

expt. no.	TCP		4-CA		4-CP		DCNB	
	CE ($\times 10^{-6}$ mg^{-2} h^{-1} L^{-2})	PE ($\times 10^{-9}$ mg L^{-1} Einstein^{-1})	CE ($\times 10^{-6}$ mg^{-2} h^{-1} L^{-2})	PE ($\times 10^{-9}$ mg L^{-1} Einstein^{-1})	CE ($\times 10^{-6}$ mg^{-2} h^{-1} L^{-2})	PE ($\times 10^{-9}$ mg L^{-1} Einstein^{-1})	CE ($\times 10^{-6}$ mg^{-2} h^{-1} L^{-2})	PE ($\times 10^{-9}$ mg L^{-1} Einstein^{-1})
1								
2	0.937	1.029	3.65	4.00	2.32	2.782	2.18	2.358
3	1.345	1.476	4.41	4.832	2.538	3.042	2.424	2.623
4	2.094	2.297	5.12	5.61	1.99	2.385	2.587	2.80
5	2.301	2.525	3.10	3.398	1.755	2.104	1.503	1.647
6	2.052	2.252	3.860	4.232	3.762	4.123	3.337	3.655
7	2.628	2.89	3.144	3.445	3.328	3.647	1.273	1.395

TABLE 3: Calculated Rate Constants (Obtained from the Slope of C_0/C versus Irradiation Time Plot) and Time Taken for Complete Degradation of 2,4,5-TCP, 4-CA, 4-CP, and 3,4-DCNB in the Presence of Catalyst and Oxidizing Agents

expt. no.	pollutant (10 ppm)	experiment with	k ($\times 10^{-2}$ h^{-1})	time taken for complete degradation (h)
1	TCP	TiO_2 (750 mg L^{-1})/H_2O_2 (20 ppm)	0.072	1.25
	TCP	$BaTiO_3$ (750 mg L^{-1})/H_2O_2(20 ppm)	0.12	1.5
2	4-CA	TiO_2 (750 mg L^{-1})/H_2O_2 (20 ppm)	0.408	0.75
	4-CA	$BaTiO_3$ (750 mg L^{-1})/APS (50 ppm)	0.22	1.25
3	4-CP	TiO_2 (750 mg L^{-1})/APS (50 ppm)	0.14	1
	4-CP	$BaTiO_3$ (750 mg L^{-1})/APS(50 ppm)	0.196	1
4	DCNB	TiO_2 (750 mg L^{-1})/APS/(50 ppm)	0.08	1.25
	DCNB	$BaTiO_3$ (750 mg L^{-1})/APS(50 ppm)	0.14	0.75

the aromatic ring; that is, halogen can both withdraw and release the electrons. It withdraws the electrons through its inductive effect and releases electrons through its resonance effect.[35] Therefore, the reactivity of the molecule is controlled by the stronger inductive effect, and orientation is controlled by the resonance effect; however, the inductive effect is stronger than the resonance effect, causing net electron withdrawal, and hence destabilizes the aromatic ring.

As per the above facts, the order of reactivity of the functional groups in the above compounds is represented in the following way: $-NH_2 > -OH > -NO_2$. Accordingly, ClAr-NH_2 is the most stable molecule, and Cl_2Ar-NO_2 is the least stable. However in the present study, the degradation process follows a slightly different order. The rate shows dependence on the nature of the intermediates formed during the irradiation.

The degradation of TCP takes place through the formation of several stable, intermediate products. Hence the complete degradation takes a longer time. In TCP molecule, the electron-withdrawing effect of −Cl is more effective in the presence of −OH group on the aromatic ring. During the photodegradation, the −Cl may be replaced by the −OH group, leading to the formation of para-substituted dihydroxy compounds, which are highly stable and take longer duration for degradation.

In the 3,4-DCNB molecule, both $-NO_2$ and −Cl groups are electron-withdrawing in nature, which strongly deactivates the ring. Therefore, 3,4-DCNB degrades at a faster rate when compared with the other molecules.

In the case of 4-CP and 4-CA, there is one electron-donating group (−OH and $-NH_2$, respectively) and one electron-withdrawing −Cl group. Therefore, the molecules are stable when compared with 3,4-DCNB and less stable than 2,4,5-TCP for the degradation.

According to G. Palmisano et al.[40,41] the nature of substituent group strongly influences: (i) the adsorption of aromatic substrate on the surface of the catalyst and (ii) the position of −OH group entering the aromatic ring giving rise to a regioselectivity in the monohydroxylated products. The adsorption of aromatic compounds containing electron-donating group on the catalyst surface is negligible. A notable adsorption is instead observed with strongly electron-withdrawing groups. The presence of

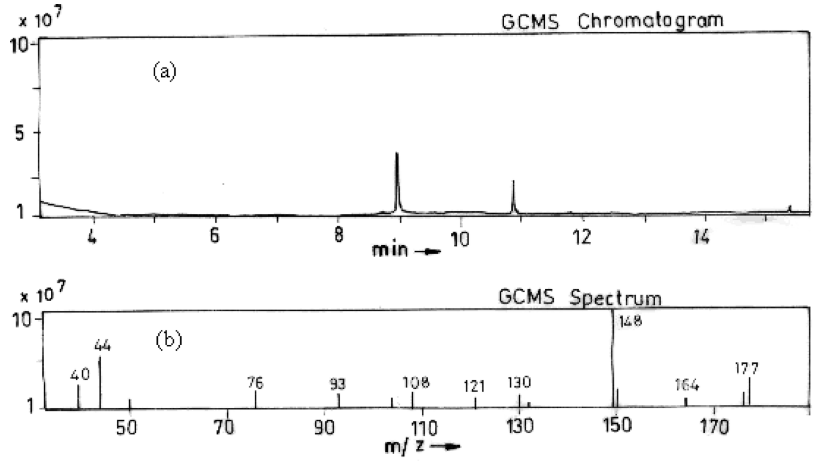

Figure 3. GC-MS spectra of 2,4,5-TCP after 0.5 h of irradiation: (a) GC and (b) MS.

certain additional electron density induced in the aromatic ring by the presence of electron-donating group is not beneficial for the molecule for adsorption. On the contrary, the presence of strongly electron-withdrawing group induces a delocalized electron density in the aromatic ring that promotes the adsorption of the molecule on the surface. The same effect supports the reaction pathway for the complete and efficient mineralization of 3,4-DCNB due to the presence of electron withdrawing $-NO_2$ and $-Cl$ groups where hydroxylation can takes place at any position. In summary, they had concluded that the reaction of monohydration of an aromatic ring occurs in all three possible positions, whereas the formation of ortho and para isomers virtually occurs when an electron-donating group is present. The observed results in our case also fall in the line of the same discussion. In the case of 2,3,5-TCP and 4-CP, the $-OH$ group is an electron-donating group and hydroxylation can take place at the para position. In the case of 4-CA, $-NH_2$ is an electron-donating group and hydroxylation was expected at the ortho or para position. However, hydroxylation initially takes place at the meta position, which is a short-lived, but subsequent hydroxylation takes place at para positions only.

In the degradation reaction, the process of both cleavage and substitution simultaneously take place in the aqueous medium. Breaking of the ring structure is less probable (not the first step) when the substituent groups are present on the aromatic ring. Furthermore, the rate of degradation of the molecules also depends on the nature and the number of the intermediates formed during degradation process.

SCHEME 1: Probable Photodegradation Reaction Mechanism of 2,3,5-TCP

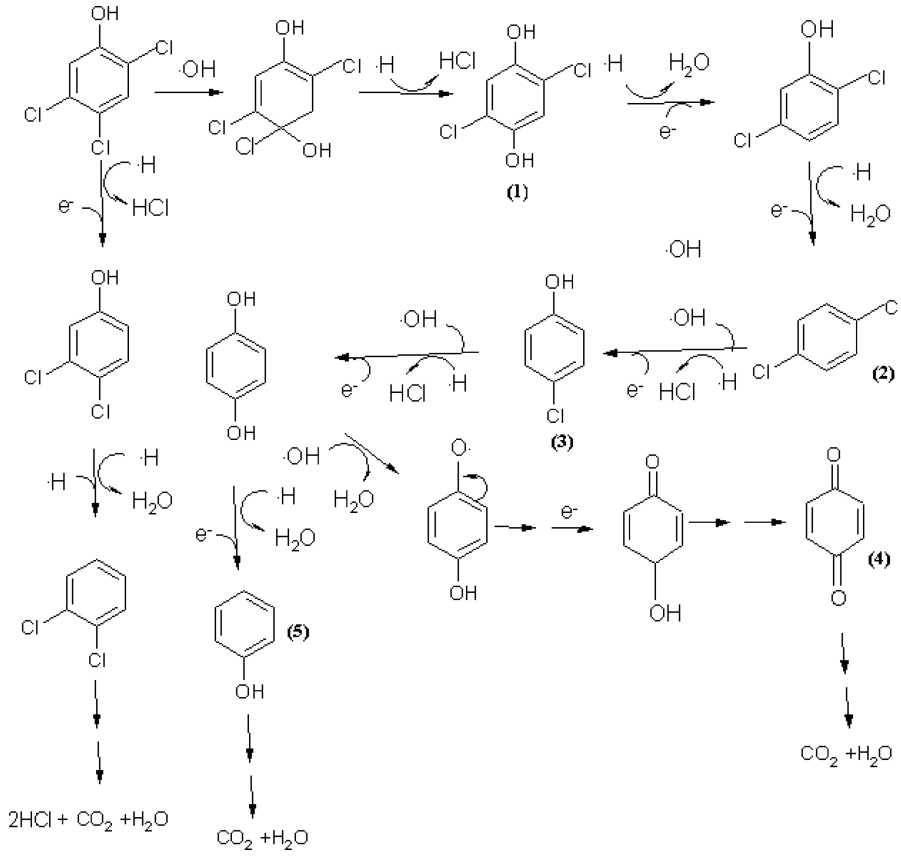

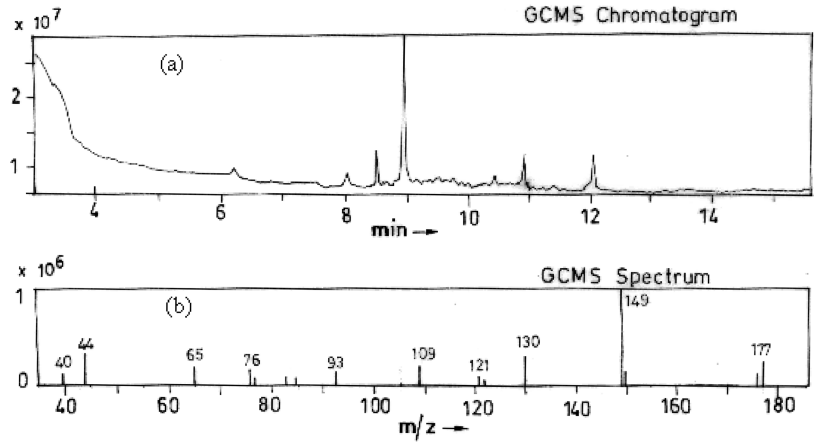

Figure 4. GC-MS spectra of 4-CA after 0.5 h of irradiation: (a) GC and (b) MS.

5. Spectroscopic Analysis. ***5.1. UV−Visible Spectral Study.*** The UV−visible absorption spectrum of the sample 2,4,5-TCP (λ_{max} = 204 nm) taken after 0.25 h of irradiation shows a small blue shift (from 300 to ~285 nm) with increased intensity, indicating the break down of the parent molecule and the formation of the intermediate compound. This band at 300 nm in the initial sample spectrum is the R-band due to the n → π^* transition of −Cl/−OH of 2,4,5-TCP.[42,43,2,3] The shift in absorption in the intermediate sample spectrum may be due to the replacement of −Cl by −OH. The spectrum of the sample after 1.5 h of irradiation does not show any absorption band, indicating the complete mineralization of TCP.

4-CA initially shows three prominent bands at 198(λ_{max}), 238, and 290 nm, which are the characteristic bands of aromatic ring with the $-NH_2$ and −Cl substituents. The intensity of the peaks decreases with illumination; finally, after 1 h of irradiation, no characteristic absorption bands were noticed in the spectrum.

The initial sample of 4-CP has three prominent absorption bands at 195(λ_{max}), 225, and 285 nm. The spectrum after 0.25 h of irradiation shows a new band at 250 nm, and the band at

SCHEME 2: Probable Photodegradation Reaction Mechanism of 4-CA

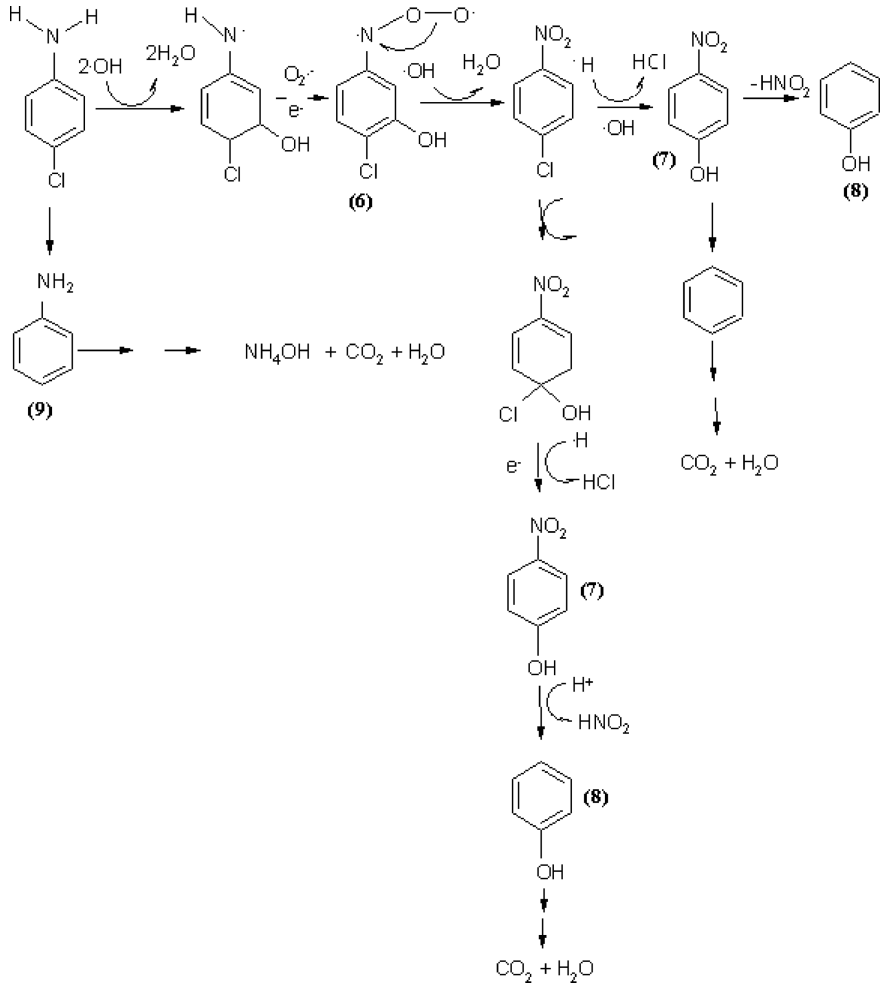

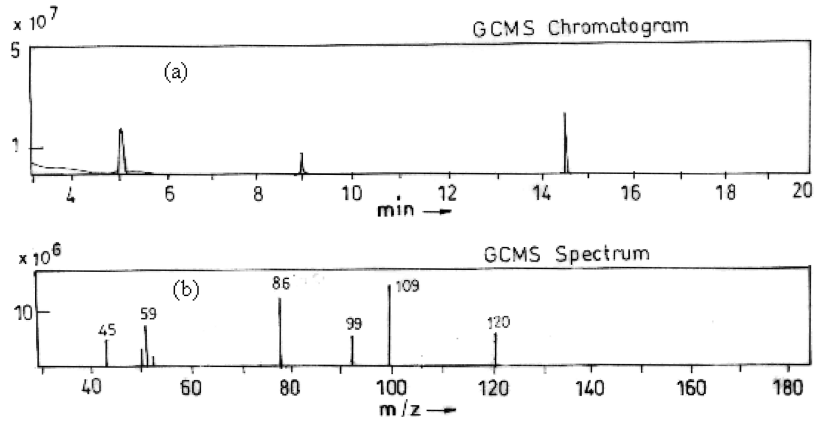

Figure 5. GC-MS spectra of 4-CP after 0.5 h of irradiation: (a) GC and (b) MS.

285 nm has completely disappeared. The former is due to the replacement of the −Cl group by the −OH group, and the latter is due to the formation of >C═O group in the molecule. Complete mineralization of 4-CP can be achieved in 1 h.

The solution of 3,4-DCNB (initial sample) has displayed two characteristic bands at 210(λ_{max}) and 275 nm. The absorption intensities of all of the bands decrease continuously on irradiation, indicating the mineralization of 3,4-DCNB.

5.2. IR Spectral Study. The details of the characteristic functional groups of the molecules are obtained from IR spectral study.[42] In the spectrum taken for 2,4,5-TCP after 0.5 h of irradiation, the peak at 3503−3462 cm^{-1} (present in the initial sample spectrum) has become more prominently wide, which could be due to substitution of −OH by the cleavage of one of the chlorine on the aromatic ring. The peak at 741 cm^{-1}completely disappears after 1 h of irradiation, indicating the cleavage of C−Cl bond of the aromatic ring.

The intermediate IR spectrum of 4-CA shows peaks at 3364 and 2919−2857 cm^{-1} after 0.5 h of irradiation due to the stretching vibrations of O−H and aromatic C−H, respectively. The peak at 1693 cm^{-1} may be assigned to C−N bending vibration of 4-hydroxy aniline, or it may be due to >C═O of quinone. The peak at 767 cm^{-1} disappears completely, indicating the cleavage of C−Cl bond.

After 0.5 h of irradiation, the intermediate IR spectrum of 4-CP clearly shows the disappearance of peak at 829 cm^{-1}, which indicates the cleavage of the C−Cl bond in the molecule. The new peak appearing at 1724 cm^{-1} can be attributed to the formation of the >C═O group of quinone.

The cleavage of the C−Cl bond (741 cm^{-1}) of 3,4-DCNB occurred in the time duration of 0.5 h of irradiation. The triplet peaks in the region 1600−1560 cm^{-1} have merged to become a prominent peak, which may correspond to the −OH group.

5.3. GC-MS Analysis. The GC-MS analysis has been carried out to confirm the intermediate products formed during the degradation process using TiO_2 and $BaTiO_3$. On the basis of the similar major intermediates formed during the process of degradation, the probable schemes have been proposed. Although there were different minor intermediates for both TiO_2 and $BaTiO_3$, the major degradation pathway is almost similar.

SCHEME 3: Probable Photodegradation Reaction Mechanism of 4-CP

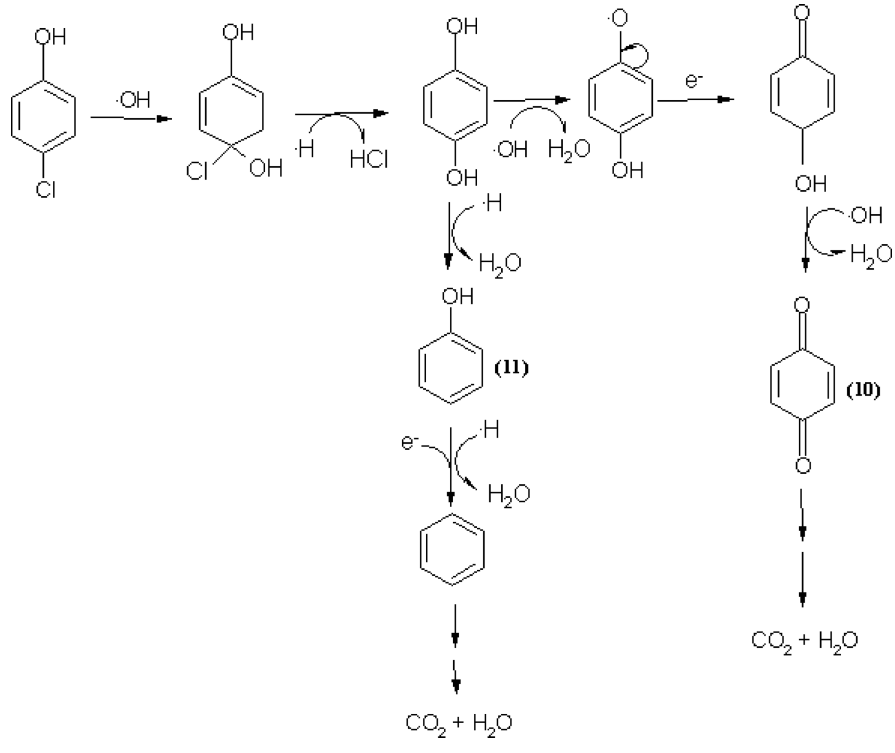

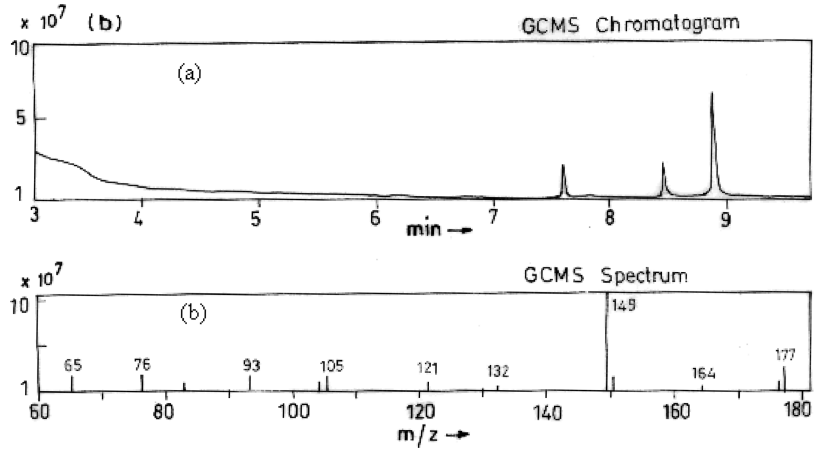

Figure 6. GC-MS spectra of 3, 4-DCNB after 0.5 h of irradiation: (a) GC and (b) MS.

SCHEME 4: Probable Photodegradation Reaction Mechanism of 3,4-DCNB

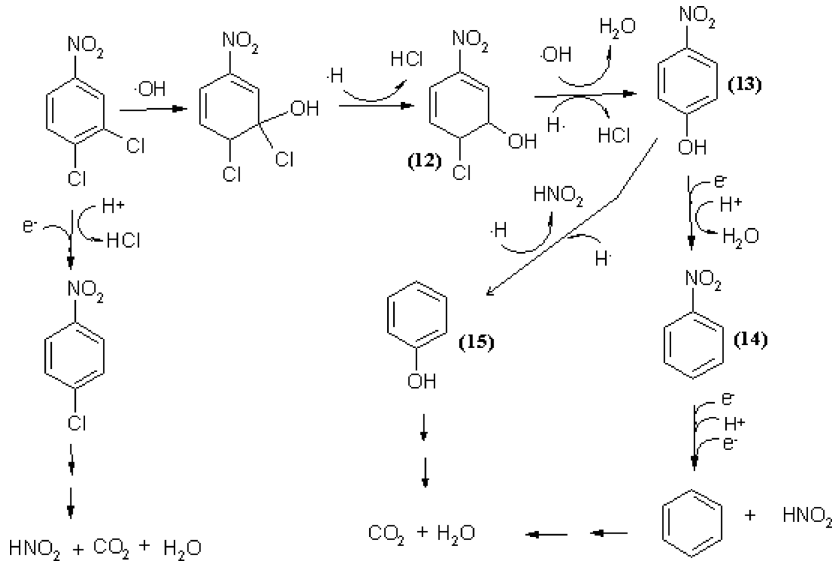

The gas chromatograph for the sample 2,4,5-TCP taken after 0.5 h of irradiation has three peaks (Figure 3a) corresponding to the retention time (R_t) values of 8.9, 11.0, and 15.45 min. The peak corresponding to the R_t value of 8.9 min has the molecular ion peak at m/z value of 177 and the base peak at m/z value of 148 (Figure 3b). This corresponds to the intermediate product (1) 2,5-dichloro-1,4-dihydroxy benzene. The other peaks in the GC spectrum correspond to the products (2) 2,5-dichlorobenzene ($m/z = 147$), (3) 4-chlorophenol ($m/z = 128$), (4) hydroquinone ($m/z = 109$), and (5) phenol ($m/z = 93$). The above intermediates are indicated in Scheme 1.

The sample of 4-CA after 0.5 h of irradiation shows four peaks at the R_t values: 8.852, 8.875, 10.946, and 12.0 min in the GC spectrum. The peak at R_t value 8.875 min in the GC spectrum corresponds to the intermediate product (6) 3-hydroxy-4-chloronitrobenzene,[43] which is a major product with the m/z value 173. The GC and mass spectra are given in Figure 4a,b respectively. The other intermediate products identified are (7) 4-hydroxy nitrobenzene ($m/z = 138$), (8) phenol ($m/z = 93$), and (9) aniline ($m/z = 92$). On the basis of the intermediates formed, a probable reaction mechanism has been proposed in Scheme 2.

The GC spectrum of the intermediate sample of 4-CP after 0.25 h of irradiation shows the new peak at the retention time 8.85 min, which corresponds to (10) hydroquinone ($m/z = 108$), a major product.[44] The GC spectrum taken at 0.5 h shows the peaks at the R_t value 4.85 min, which corresponds to the product (11) phenol ($m/z = 93$). Figure 5a,b corresponds to GC and mass spectra of 4-CP, respectively. Compounds 10 and 11 are indicated in the Scheme 3.

The GC spectrum of the sample of DCNB after 0.5 h of irradiation has the peaks at the R_t values 7.67, 8.48 and a strong peak at 8.892 min. The mass spectrum has given the molecular ion peak for the intermediate product at the m/z value 173 and the base peak at the m/z value 149 (Figure 6a,b). It shows that one of the products (12) formed is 3-hydroxy-4-chloronitrobenzene. The other products identified are (13) 4-hydroxy nitrobenzene ($m/z = 138$), (14) nitrobenzene ($m/z = 123$), and (15) phenol ($m/z = 93$). The reaction mechanism is represented in the Scheme 4.

Some of the intermediate products formed from the above chloroorganic compounds are found to be the same. For example, the intermediate compounds 5, 8, 11, and 15 correspond to phenol, 4 and 10 correspond to hydroquinone, 6 and 12 correspond to 3-hydroxy-4-chlorobenzene, and 7 and 13 correspond to 4-hydroxy nitrobenzene. Although the same products are observed, the reaction pathways are found to be completely different. The above mechanisms proposed in the present research are for $TiO_2/BaTiO_3$. The schemes have been proposed on the basis of the similar major intermediates formed during the process of degradation, which could be identified. Although there were different unidentified minor/major inter-

mediates for both TiO_2 and $BaTiO_3$, the major degradation pathways are the schemes that we have proposed in each case.

Conclusions

Higher catalytic efficiency and quantum yields are observed for the perovskite wide band gap semiconductor $BaTiO_3$, especially in the presence of ammonium persulphate when compared with TiO_2. This can be accounted because of (i) the favorable coordination environment of surface atoms, (ii) red-ox properties of the oxides, and (iii) oxidation state of the metal ions at the surface of the photocatalyst. These conditions seem to be more favorable for $BaTiO_3$ when compared with TiO_2. Another important factor that can influence the degradation rate is pH, which in turn influences the catalytic and process efficiencies. The pH can alter the band edge potentials/red-ox potentials of the semiconductor-substrate system in the reaction solution. The efficient degradation of the above chloroorganic compounds is achieved in alkaline medium.

The rate of photocatalytic degradation of the target chloro-organic compounds is of the order TCP < 4-CA < 4-CP < DCNB. A higher rate is observed for the degradation of DCNB, whereas TCP is found to be more stable for degradation. The 4-CP and 4-CA shows almost equal resistance for the degradation when compared with DCNB. TCP shows more resistance for the degradation among these molecules because it contains an electron-releasing −OH group and three electron-withdrawing −Cl groups. The deactivating nature of −Cl atoms is more in TCP compared with 4-CP and 4-CA. Therefore the stability of the aromatic ring is expected to be low in TCP, but TCP degrades at slower rate compared with the other compounds because one of the chlorines (ortho to −OH) is replaced by a −OH group in the immediate intermediate that makes the molecule more stable. Later, the cleavage of both of these −OH groups leads to the formation of *para*-dichlorobenzene. Furthermore, it is converted to *para*-dihydroxybenzene. Therefore, degradation takes place via the formation of a greater number of stable intermediates. Hence the complete degradation of TCP takes longer time compared with that of other compounds. In addition to this, the resonance effect of −Cl atoms (electron releasing nature) to some extent may stabilize the aromatic ring. This can be another cause for the slower rate of degradation of TCP.

The chloroaromatic compounds with more electron-donating groups (−OH, $-NH_2$, etc.) are found to be more resistant for degradation, and those having an electron-withdrawing group like $-NO_2$ tend to degrade at a faster rate. The intermediate products formed during the degradation of these compounds have been identified, and the probable reaction mechanisms have been proposed.

Acknowledgment. We would like to acknowledge UGC and DST, Government of India.

References and Notes

(1) (a) Yu, J.; Yu, H.; Cheng, B.; Trapalis, C. *J. Mol. Catal. A: Chem.* **2006**, *249*, 135–142. (b) Yu, J.; Zhang, L.; Cheng, B.; Su, Y. *J. Phys. Chem. C* **2007**, *111*, 10582–10589. (c) Yu, J.; Liu, W.; Yu, H. *Cryst. Growth Des.* **2008**, *8*, 930–934. (d) Yu, J.; Su, Y.; Cheng, B. *Adv. Funct. Mater.* **2007**, *17*, 1984–1990. (e) Yu, J.; Wang, G.; Cheng, B.; Zhou, M. *Appl. Catal., B* **2007**, *69*, 171–180.

(2) (a) Tanaka, S.; Saha, U. K. *Water Sci. Technol.* **1994**, *30*, 47–57. (b) Mills, A.; Davies, R. *J. Photochem. Photobiol., A* **1995**, *85*, 173–178.

(3) Pera-Titus, M.; Garcia-Molina, V.; Banos, M. A.; Gimenez, J.; Esplugas, S. *Appl. Catal., B* **2004**, *47*, 219–256.

(4) (a) Gomathi Devi, L.; Krishnamurthy, G. *J. Hazard. Mater.* **2009**, *162*, 899–905. (b) Gomathi Devi, L.; Krishnamurthy, G. *J. Environ. Sci. Health, Part B* **2008**, *43*, 553–561.

(5) Meng, Y.; Huang, X.; Wu, Y.; Wang, X.; Qian, Y. *Environ. Pollut.* **2002**, *117*, 307–313.

(6) Mogyorósi, K.; Farkas, A.; Dékány, I.; Ilisz, I.; Dombi, A. *Environ. Sci. Technol.* **2002**, *36*, 3618–3624.

(7) Lin, L.; Kuntz, R. R. *J. Photochem. Photobiol., A* **1992**, *66*, 245–251.

(8) Prager, L.; Hartmann, E. *J. Photochem. Photobiol., A* **2001**, *138*, 177–183.

(9) Serpone, N., Pellizetti, E. *Photocatalysis: Fundamentals and Applications*; Serpone, N., Pelizzetti, E., Eds.; Wiley: New York, 1989.

(10) Matthews, R. W.; McEvoy, S. R. *J. Photochem. Photobiol., A* **1999**, *66*, 355–366.

(11) Saquib, M.; Muneer, M. *Dyes Pigm.* **2002**, *53*, 237–249.

(12) *The Condensed Chemical Dictionary*, 10th ed.; Van Nostrand Reinhold: New York, 1981.

(13) Gomathi Devi, L.; Krishnaiah, G. M. *J. Photochem Photobiol., A* **1999**, *121*, 141–145.

(14) Padmini, P.; Kutty, T. R. N. *J. Mater. Chem.* **1994**, *4*, 1875–1881.

(15) Fuller, M. P.; Griffiths, P. R. *Anal. Chem.* **1978**, *50*, 1906–1910.

(16) Mill, A.; Valezulea, M. A. *J. Photochem. Photobiol., A* **2004**, *165*, 25–34.

(17) Mills, A.; Le Hunte, S. *J. Photochem. Photobiol., A* **1997**, *108*, 1.

(18) Bahnemann, D. W.; Bockelmann, D.; Goslich, R. *Sol. Energy Mater.* **1991**, *24*, 564–583.

(19) Braun, A. M.; Maurelte, M. T.; Oliveros, E. *Photochemical Technology*; Wiley: New York, 1991.

(20) Devi, L. G.; Girish, K. S.; Mohan, R. K. *Cent. Eur. J. Chem.* **2009**, *7*, 468–477.

(21) Fox, M. A.; Dulay, M. T. *Chem. Rev.* **1993**, *93*, 341–357.

(22) Klaning, W. K.; Sehested, K.; Wolff, T. *J. Chem. Soc., Faraday Trans 1* **1984**, *80*, 2969.

(23) (a) Houas, A.; Lachheb, H.; Ksibi, M.; Elaioui, E.; Guillard, C.; Herrmann, J. M. *Appl. Catal., B* **2001**, *107*, 4545. (b) Devi, L. G.; Kottam, N.; Kumar, S. G. *J. Phys. Chem. C* **2009**, *113*, 15593–15601.

(24) Zhang, T.; Oyama, T.; Horikoshi, S.; Zhao, J.; Serpone, N.; Hidaka, H. *Appl. Catal., B* **2003**, *42*, 13–24.

(25) Kamat, P. V. *Chem. Rev.* **1993**, *93*, 267–300.

(26) Wang, K.; Zhang, J.; Lou, L.; Yang, S.; Chen, Y. *J. Photochem. Photobiol., A* **2004**, *165*, 201–207.

(27) Riga, A.; Soutsas, K.; Ntampegliotis, K.; Karayannis, V.; Papapolymeru, G. *Desalination* **2007**, *211*, 72–86.

(28) Devi, L. G.; Murthy, B. N. *Catal. Lett.* **2008**, *125*, 320–330.

(29) Alhakimi, G.; Gebril, S.; Studnicki, L. H. *J. Photochem Photobiol., A* **2003**, *157*, 103–109.

(30) da Silva, C. G.; Faria, J. L. *J. Photochem Photobiol., A* **2003**, *155*, 133–143.

(31) Xu, T.; Xiao, X.-M.; Liu, H.-Y. *J. Environ. Sci. Health, Part A* **2005**, *40*, 751–765.

(32) Wang, X. H.; Li, J.-G.; Kamiyama, H.; Moriyoshi, Y.; Ishigaki, T. *J. Phys. Chem. B* **2006**, *110*, 6804–6809.

(33) Laidler, K. J. *Chemical Kinetics*, 3rd ed.; Harper & Row: New York, 1987.

(34) Laidler, K. J. *Chemical Kinetics*, 2nd ed.; Tata-McGraw Hill: New Delhi, India, 1973.

(35) Ramand, C. *Physical Chemistry with Applications to Biological Systems*; Macmillan: New York, 1977.

(36) Devi, L. G.; Murthy, B. N.; Kumar, S. G. *J. Mol. Catal. A: Chem.* **2009**, *308*, 174–181.

(37) (a) Zaharaa, O.; Sauvanaud, L.; Hamard, G.; Bouchy, M. *Int. J. Photoenergy* **2003**, *5*, 87–93. (b) Wang, X. H.; Li, J.-G.; Kamiyama., H.; Moriyoshi, Y.; Ishigaki, T. *J. Phys. Chem. B* **2006**, *110*, 6804–6809.

(38) Wanaratna, P.; Christodoulatos, C.; Sidhoum, M. *J. Hazard. Mater.* **2006**, *136*, 68–74.

(39) Morrison, R. T.; Boyd, R. N. *Organic Chemistry*, 6th ed.; Prentice-Hall of India Private Limited: New Delhi, India, 1999.

(40) Palmisano, G.; Addamo, M.; Augugliaro, V.; Caronna, T.; Paola, A. D.; Garcia-Lopez, E.; Loddo, V.; Palmisano, L. *Chem. Commun.* **2006**, 1012–1014.

(41) Palmisano, G.; Addamo, M.; Augugliaro, V.; Caronna, T.; Garcia-Lopez, E.; Loddo, V.; Marci, G.; Palmisano, L.; Schiavello, M. *Catal. Today* **2007**, *122*, 118–127.

(42) (a) Silverstein, R. M.; Bassler, G. C.; Morrill, T. C. *Spectrometric Identification of Organic Compounds*, 4th ed.; John Wiley & Sons: New York, 1981. (b) Dyer, R. J. *Applications of Absorption Spectroscopy of Organic Compounds*; Prentice-Hall of India Pvt. Ltd.: New Delhi, India, 1965.

(43) Legrini, O.; Oliveros, E.; Braun, A. M. *Chem. Rev.* **1993**, *93*, 671–698.

(44) Linsebigler, A. L.; Lu, G.; Yates, J. T., Jr. *Chem. Rev* **1995**, *95*, 735–758.

JP103301Z